Progress in the Application of SERS Technology in Monitoring Endogenous Metabolites and Drug Metabolism

Peipei Chen

First People's Hospital, Xiaoshan District, Hangzhou, Zhejiang 310000, China

wmu.cpp@outlook.com

Abstract

Raman spectroscopy, as a "fingerprint" technique for molecular structure analysis, is difficult to apply directly for trace detection due to its weak signal. Surface-enhanced Raman spectroscopy (SERS) amplifies the signal through plasmonic resonance, offering a feasible solution for dynamic monitoring of small molecule drugs and metabolites in biological fluids. This paper briefly introduces the mechanism of SERS, details how SERS can be combined with sensor technologies and machine learning to enhance the sensitivity and reproducibility of metabolite detection, and provides specific design ideas and innovations for applications. Additionally, the diversity of SERS applications in drug detection is presented, ranging from precise drug quantification in serum to drug metabolism dynamics studies within cells, and the development of SERS technology for monitoring exosome drug-loading rates. Finally, the paper discusses the current status of SERS technology in detection and potential future directions for development.

Keywords

SERS; Metabolite Detection; Drug Monitoring.

1. Introduction

During cellular metabolic activities, thousands of metabolites are produced. Over many years, these nutrients have been defined and compiled into a map containing approximately 20 metabolic pathways [1]. Metabolites refer to the sum of precursors, intermediates, and end products in cellular metabolic activities, providing energy and precursor substances for biosynthesis [2]. Metabolites interact with protein receptors expressed on tissues, cells, and glands to transmit cellular signals, regulating cell growth, differentiation, and metabolism [3]. Metabolites can also act as cofactors for chromatin-modifying enzymes and modulate gene regulatory proteins, linking metabolic information with transcriptional programs[4, 5]. This illustrates the importance of metabolites in cellular physiological functions and biological health.

Metabolic disorders are seen in diseases such as obesity, diabetes, respiratory diseases, cardiovascular diseases, and cancer. Although genes are considered the root cause, they only explain part of the disease. The exclusive metabolic profiles and biomarkers produced by the interaction between genetics and the life environment are used for disease screening, early diagnosis, and therapeutic interventions [6, 7]. Metabolites, due to their small molecular weight and simple structure, can be analyzed and identified using high-sensitivity techniques. Numerous studies have demonstrated significant differences in metabolite profiles between patients and healthy individuals in body fluids [8, 9]. The types of body fluids primarily studied include non-invasive samples such as urine and feces, as well as minimally invasive samples like blood, cerebrospinal fluid, pleural and peritoneal fluid, and bile, all of which greatly satisfy the need for repeatable monitoring.

It is well known that cancer cells require a large amount of energy, which alters metabolic pathways, the expression of important intermediates, and related enzymes, resulting in specific metabolic tendencies and dependencies. Understanding the proportional impact of different metabolites in disease progression can create therapeutic opportunities [10]. Typical disease-related metabolites include lipids, amino acids, nucleic acid bases, sugars, and vitamins. First, glucose metabolism: in the 1920s, Otto Warburg first observed that cancer cells consume more glucose to produce lactate under aerobic conditions. Although ATP generated by glycolysis is less than that from oxidative phosphorylation, glycolysis has a faster ATP synthesis rate, which is suitable for rapidly proliferating cells. Additionally, glycolysis intermediates can be used to synthesize large molecules necessary for cancer development and proliferation. The pentose phosphate pathway (PPP) is also a key source of the antioxidant NADPH, helping cells adapt to changes in their microenvironment [10, 11]. In normal adult cells, de novo synthesis of free fatty acids (FA) is low, but in glioblastoma, breast cancer, ovarian cancer, lung cancer, prostate cancer, and liver cancer, all three enzyme families involved in FA synthesis (ACC, FXR, SCD) are frequently upregulated, leading to increased lipid production, which helps cancer cells build phospholipid-rich cell membranes. Furthermore, lipid metabolites also play roles in cell signaling and protein transport, which are critical in tumor proliferation and metastasis [12, 13].

Amino acids are frequently mentioned as biological molecules that provide the raw material for proteins. They are the direct basis for diagnosing many congenital metabolic diseases. For instance, phenylketonuria (PKU) is caused by a metabolic enzyme defect, leading to the accumulation of phenylalanine and its intermediates, which toxicologically damage the central nervous system and cause intellectual disability. Branched-chain amino acids are associated with insulin resistance and obesity. Under isocaloric conditions, long-term increases in the ratio of branched-chain amino acids to other amino acids in the diet promote appetite, leading to obesity[14]. Studies have even shown that amino acids can support immune cell metabolic reprogramming [15].

Additionally, the pharmacokinetics of exogenous drugs in the body have attracted considerable attention. For example, critically ill patients require careful monitoring of anti-infective drug doses in the blood due to pathological and physiological factors[16]. Variations in drug-metabolizing enzymes, drug transporters, and drug target genes lead to individualized drug efficacy. The best strategy is to monitor drug metabolism in real-time, improve therapeutic efficacy, and reduce adverse drug reactions. After deciphering the metabolic pathways of biomolecules and related physiological functions, researchers can target and use metabolites as tools for drug development [17]. Therefore, whether endogenous or exogenous metabolites, monitoring the dynamic changes of these biomolecules helps understand life processes and disease evolution mechanisms.

For the detection and identification of the metabolites and drugs mentioned above, numerous characterization methods have been applied. Raman spectroscopy is a highly sensitive, non-destructive, and rapid detection technique, but weak scattering signals have limited its widespread use. In 1974, Fleischmann first observed significantly enhanced Raman signals on the rough surface of silver electrodes [18]. With the elucidation of the signal enhancement mechanism, subsequent improvements, such as tip-enhanced Raman spectroscopy and shell-isolated nanoparticle-enhanced Raman spectroscopy, have largely addressed material and morphology universality issues. Therefore, the non-destructive, non-contact detection features of surface-enhanced Raman spectroscopy (SERS) have expanded its application from environmental materials to biomedicine[19, 20]. For example, Wang et al. used SERS to monitor bioactive metabolites produced by ampicillin-resistant *Pseudomonas aeruginosa* strains and identified the underlying resistance mechanisms[21]; Yu et al. observed distinct and highly enhanced SERS peaks from semipolar aromatic metabolites in pancreatic cancer

and prostate cancer samples, and used SERS fingerprint spectra for urine metabolite analysis to successfully differentiate pancreatic cancer and prostate cancer groups from normal controls [22].

Based on the aforementioned studies, this paper focuses on recent advances in SERS technology for monitoring endogenous metabolites and drug metabolism in humans, compares and analyzes the characteristics and innovative ideas of various studies, and summarizes the current challenges and potential future directions of SERS technology.

2. SERS Mechanism

SERS is the interaction process between incident laser light, metallic nanoparticles, and molecular Raman scattering. Understanding the SERS enhancement mechanism can guide precise experimental design, providing highly sensitive and reliable detection results [23]. The primary mechanisms for signal amplification are electromagnetic field enhancement (EM) and chemical enhancement (CM). The contribution of each mechanism has been quantified, with the EM mechanism dominating, having a clear physical basis and being widely accepted and successfully applied [24].

First, light illuminates the molecule, and the frequency of the incident light and reflected light are the same, which is Rayleigh scattering. After the light interacts with the molecule, energy is exchanged, and the reflected light frequency differs from the incident light, resulting in Raman scattering. The molecule absorbs energy from photons and emits light at a frequency lower than that of the incident light. This type of Raman scattering is called Stokes scattering, while the opposite is called anti-Stokes scattering [25], as shown in Figure 1a. Under normal conditions, Raman scattering signals are very weak, and the EM enhancement principle is that when the frequency of the incident laser matches the fixed vibration frequency of free electrons in metal nanoparticles like gold, silver, copper, etc., surface plasmon resonance (LSPR) occurs, as shown in Figure 1b. The resonance state causes free electrons to accumulate on the nanoparticle surface, increasing the surface charge density and enhancing the local electromagnetic field strength by 2-5 orders of magnitude. When the molecule to be measured is placed in the enhanced local field, the Raman signal is significantly amplified. The entire process is divided into two steps: The first step is when the molecule undergoes enhancement in the surface local field E_{local} at the excitation wavelength, expressed by the factor $M_{ex}=|E_{local}(w_0)/E_0(w_0)|^2$ (where w_0 is the incident light frequency, E_0 is the incident light). The second step is that plasmonic nanoparticles transfer the Raman signal from near-field to far-field, with the Raman signal enhancement being positively correlated with the local electric field at the emission wavelength, expressed by the factor $M_{sc}=|E_{local}(w_{sc})/E_0(w_{sc})|^2$ (where w_{sc} is the scattering frequency), so the final enhancement effect is the result of both excitation and radiation, represented by the expression $M=M_{ex}\times M_{sc}$ [26]. The SERS enhancement intensity can be roughly calculated using the formula $(1 + r/a)^{-12}$, where r is the distance between the molecule and nanoparticle surface, and a is the nanoparticle radius. It can be seen that the intensity drastically decreases as the distance between the molecule and nanoparticle increases [24, 25]. Therefore, one can increase the affinity between target molecules and nanomaterials by adding chemical and physical modifications to the metal nanoparticle surface, which helps enhance the SERS signal and improves the uniformity of the substrate material, thus enhancing the reproducibility of the SERS signal and ultimately improving sensitivity [27].

Although individual nanoparticles already improve the signal strength considerably, when two metal nanoparticles are brought extremely close to each other, a stronger electromagnetic field is generated in the gap between them, leading to a signal increase by several orders of magnitude. This gap is referred to as a “hotspot,” as shown in Figure 1c.

Using this principle, rational designs of nanoparticle size, shape, and coating can efficiently amplify the signal of the molecules to be measured. It is noteworthy that even a few nanometers away from the hotspot region leads to a drastic decrease in signal strength. Additionally, the limited number of hotspots and their random distribution in nanomaterials can also affect the accuracy of both quantitative and qualitative results. The above information also emphasizes that the design of nanoparticle substrate materials and assembly structures is crucial for the detection process and SERS data interpretation [24].

Unlike EM, CM entirely depends on the molecular properties and can directly alter the spectral pattern, including peak position and intensity, with an estimated enhancement factor ranging from 10-100 times. The key to the CM mechanism is the change in molecular polarizability. When a molecule adsorbs onto the metal surface, the redistribution of the electron cloud and the interaction between the metal and the molecule can change the molecular polarizability. Additionally, when the highest occupied molecular orbital or lowest unoccupied molecular orbital of a molecule matches the energy difference with the metal Fermi level and excitation wavelength, charge transfer may occur, increasing the molecular polarizability and ultimately altering the Raman signal [26]. After understanding the working principle behind SERS, the next section will discuss its applications in metabolites and drugs.

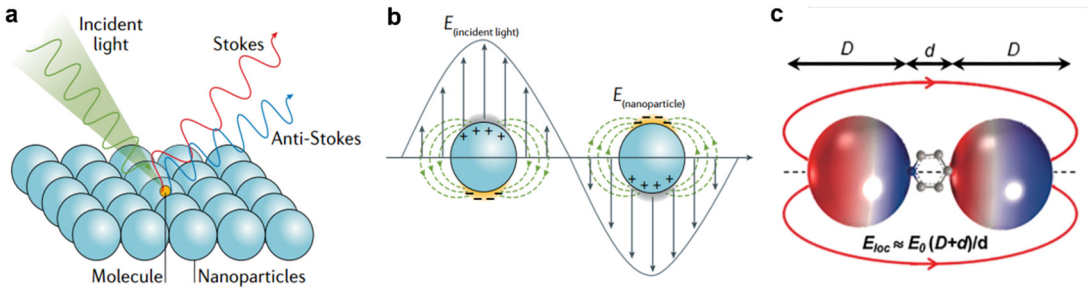


Figure 1. (a) Stokes and anti-Stokes scattering formed by molecules on the surface of nanoparticles. (b) Localized surface plasmon resonance (LSPR) phenomenon [23]. (c) "Hotspot" generated between nanoparticle aggregates [24].

3. SERS Detection of Metabolites and Drug Monitoring

SERS technology exhibits a "long-range effect," where certain biomolecules cannot be anchored on the nanoparticle surface due to reasons such as low concentration of small molecule metabolites in complex matrices, high background noise, and the lack of special chemical characteristics that can be tagged. When detecting the target substance, it heavily relies on the signal amplification strategy of an active substrate. Fabricating SERS substrates that simultaneously exhibit high sensitivity, uniformity, and reproducibility remains a challenge. The application design can generally be divided into label-free and label-mediated SERS methods. Label-free SERS detection directly utilizes biomolecules near the enhanced nanoparticle local field for signal amplification. This approach is very simple, time-efficient, and, when combined with portable Raman instruments, is suitable for rapid analysis. The other method is the indirect detection using a labeled SERS nanoprobe, where the typical nanoprobe structure generally includes: (1) metal nanoparticles as substrates that generate LSPR, (2) surface-modified molecules or characteristic groups, (3) a protective layer to stabilize the nanoparticles, and (4) a targeting biological ligand [28-30]. These unique design solutions will be discussed in detail in the following sections.

3.1. SERS and Biosensing Technology

SERS biosensing technology uses biological molecules as sensitive elements, with the signals of molecular interactions with the substrate expressed in optical, electrical, or magnetic fields. Typically, metal nanoparticles are embedded in medium-sensing materials. To facilitate easy wearing, current-sensing medium materials have shifted from rigid substrates such as glass slides and silicon wafers to flexible materials like paper, cotton, and films. Zhao et al. used MXene (Ti_3C_2TX) as the base material, uniformly adsorbing Au@Ag nanoparticles to construct high-density "hotspots" and combining them with polyvinyl alcohol (PVA) hydrogel materials to form composite substrates (TA-H) for multiple analyses of sweat metabolites, as shown in Figures 2a and 2b. Additionally, Figure 2c shows the SERS spectra of uric acid and creatinine standard solutions and synthetic sweat. The synthetic sweat spectrum displays distinct Raman peaks for uric acid and creatinine at 635 cm^{-1} and 680 cm^{-1}, respectively. The sensor has quantitative detection ranges for uric acid (10^{-4}–10^{-8} M) and creatinine (10^{-3}–10^{-6} M), with calibration curve correlation coefficients of 0.981 and 0.975, respectively, indicating good linear relationships. Furthermore, the sensor showed minimal signal fluctuation after 200 bending cycles under volunteer wear [31].

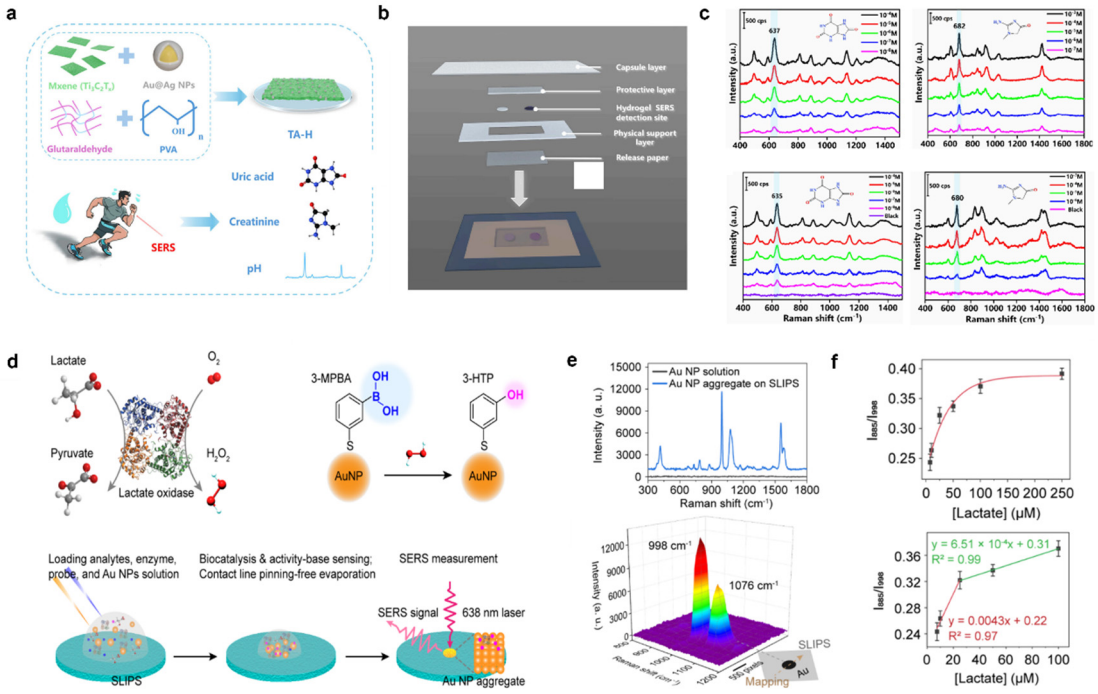


Figure 2. (a) Schematic diagram of abSLIPSERS detection (b) Internal structure diagram of wearable SERS sensor (c) SERS spectra of uric acid creatinine standard solution and synthetic sweat [31] (d) Schematic diagram of lactate detection by abSLIPSERS (e) SERS spectra of 3-MPBA detected on gold nanoparticle solution and SLIPS substrate, with SERS mapping showing enrichment of gold nanoparticles and 3-MPBA on the SLIPS substrate (f) Relative intensity spectra (I_{885}/I_{998}) vs. lactate concentration graph and linear curve of relative intensity spectra (I_{885}/I_{998}) vs. lactate concentration (7.5–100 μM) [32]

Another design idea is to combine sensors with enzymatic reactions. According to incomplete statistics, approximately 100 types of medical metabolites can be catalyzed by specific enzymes to produce quantifiable H_2O_2. Cai et al. designed a novel SERS sensor (abSLIPSERS), which does not require the synthesis of a nanoprobe, avoiding reproducibility fluctuations caused by batch-to-batch differences. In the experiment, the target metabolite, specific

oxidase, and unlabeled Au nanoparticles, along with phenylboronic acid salt, are mixed. The metabolic reaction with the enzyme produces quantifiable H_2O_2, which oxidizes 3-mercaptophenylboronic acid (3-MPBA) to form 3-hydroxyphenylthiol (3-HTP). This process is accompanied by the appearance of a characteristic Raman peak at 885 cm^{-1}. Ultimately, SLIPSERS drives self-concentration and completes the function of reading metabolite information, as shown in Figure 2d. To test the SERS activity of the Au assembly, a suspension of Au NPs containing 10 mM 3-MPBA was detected via SLIPSERS. The spectrum in Figure 2e shows the high signal-to-noise ratio of 3-MPBA (998 cm^{-1}) molecular spectral fingerprints after SLIPSERS. This indicates that SLIPSERS indeed has the function of pre-concentrating samples. Additionally, the platform measured standard lactate solutions ranging from 7.5 to 250 μM, with SERS intensity (I_{885}/I_{998}) increasing as lactate concentration increased (Figure 2f). The calibration curve shows a two-phase linear relationship (7.5–25 μM and 25–100 μM), with good linearity. To demonstrate its effectiveness in analyzing clinical biofluids, the sensor was tested on serum samples from non-small cell lung cancer (NSCLC) patients (n=33) and healthy controls (n=22). The SLIPSERS fingerprint spectra of the 55 sample cohort revealed that the serum metabolite levels of lactate and choline were decreased in NSCLC patients, while glucose levels were elevated, providing new diagnostic insights for lung cancer. The abSLIPSERS sensor is a promising analytical tool for disease diagnosis [32].

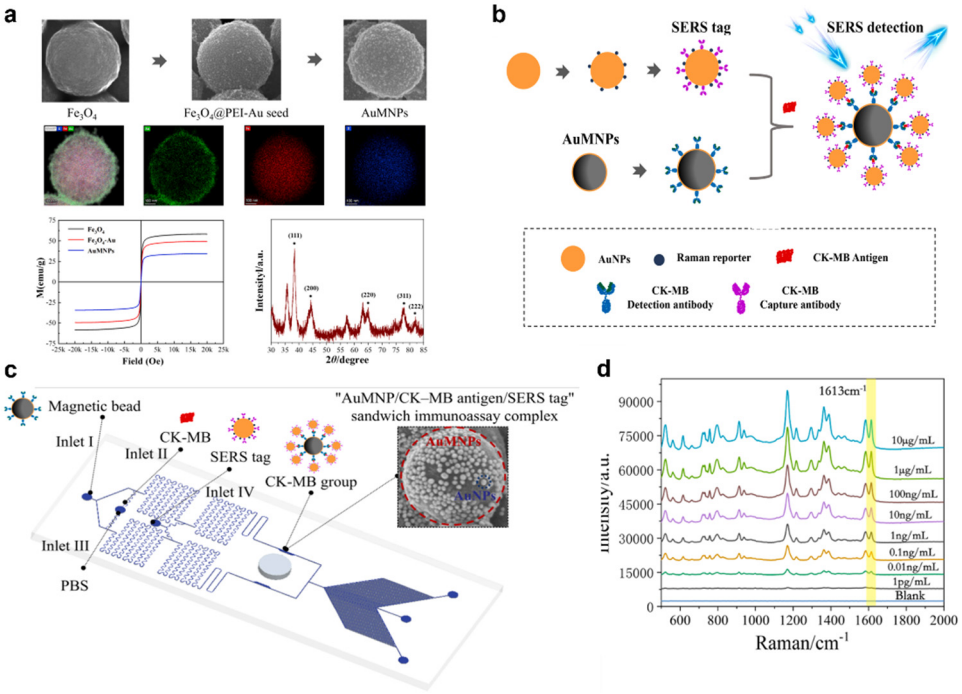


Figure 3. (a) SEM, TEM, VSM, and XRD test results of Au-MNP (b) Schematic diagram of sandwich immunocomplex formed by Au-MNP and CK-MB along with MGITC-functionalized gold nanoparticles (c) Schematic diagram of microfluidic chip detecting CK-MB (d) SERS spectra of CK-MB at different concentrations [33].

SERS sensor-related technologies have simplified the operation of SERS, offering fast testing speed, miniaturization, portability, and are particularly well-suited for integration with on-site testing scenarios. During myocardial injury, creatine kinase isoenzyme (CK-MB) starts to rise 3-4 hours after the onset and is an important biomarker for myocardial infarction. These metabolites need to be detected immediately at the onset of symptoms. Currently, the detection equipment is expensive and typically performed by specialized technicians at specific locations. In this context, Dong et al. utilized an antigen-antibody matching strategy to

implement multiple functions on a microfluidic chip platform integrated with SERS, which completes sample preprocessing, complex formation, enrichment, and detection on the same platform. First, the magnetic capture probe Au-MNP was synthesized using the ultrasonic-assisted hydroxylamine seeding growth method. Scanning electron microscopy (SEM), transmission electron microscopy (TEM), and X-ray diffraction (XRD) spectra (Figure 3a) all show dense, uniform Au-coated Fe_3O_4 nanoparticles, with preserved magnetic properties. When the sample flows through the capillary microchannel, both the magnetic capture probe (Au-MNP) and the reporter probe (MGITC-functionalized gold nanoparticles) bind with CK-MB in the sample, forming a sandwich immunocomplex. Under the action of a gradient magnetic field, the complex is captured and enriched in the detection chamber. The testing process is shown in Figures 3b and 3c. The concentration of CK-MB is directly proportional to the SERS signal intensity at the 1613 cm^{-1} characteristic Raman peak, as shown in Figure 3d. The chip still exhibits a significant signal at a CK-MB concentration of 1 pg/ml, well below the clinical positive range. The advantage of this method is that the entire process, sample introduction, immunocomplex formation, and in-situ SERS detection, is automated, allowing for precise CK-MB detection in under 15 minutes, achieving early and accurate diagnosis of acute myocardial infarction (AMI) [33].

3.2. Machine Learning (ML) Assisted SERS

The signal data collected after SERS analysis is quite large, and interpreting the overlapping peak signals in vibrational fingerprint spectra, along with background noise and sample differences, presents significant challenges. To handle these complex data, current studies often integrate machine learning (ML) algorithms and multivariate statistical analysis with SERS to extract and predict better results. More importantly, through data learning, ML can be applied to disease screening and classification for unknown samples.

ML consists of a series of geometric-based methods that can be used to predict the properties of molecules and materials. It not only processes local peak signals but also offers high automation for experimental data preprocessing. Moreover, ML can generate more varied datasets, including principal component analysis (PCA), random forest (RF), partial least squares (PLS), quadratic discriminant analysis (QDA), and partial least squares discriminant analysis (PLS-DA), which can effectively explain the differences between data groups [34, 35]. Zhu et al. used label-free SERS technology to quantitatively detect target metabolites such as glucose, uric acid, and lactate in sweat. They also integrated metabolic profiles with ML to establish six analytical models, including SVM, XGBoost, KNN, Logistic Regression, CNN, and DNN, to classify physiological states. The visual heat map showed that the SVM model performed the best, thanks to the non-linear kernel function and maximum margin principle of support vector machines, making it suitable for classification in high-dimensional overlapping feature spaces. XGBoost and CNN followed, with each model showing relative strengths and weaknesses, indicating the remarkable performance of ML in handling complex matrix sample data [36]. Additionally, multivariate statistical analysis methods are frequently combined to analyze SERS data. Shafique et al. used partial least squares regression (PLSR) and principal component analysis (PCA) to further confirm the classification and screening capabilities of SERS. PLSR has the ability to quantify SERS signals into concentrations and was used for quantitative analysis of high triglyceride and high cholesterol samples. The root mean square error of calibration (RMSEC) for the PLSR model was 5.78 mg/dl, and the root mean square error of validation (RMSEV) was 6.04 mg/dl, indicating the feasibility of the model [37]. In summary, SERS technology guided by ML shows great potential in disease screening, monitoring, and personalized medical treatment.

3.3. SERS for Drug Monitoring

With the spread of therapeutic drug monitoring concepts, clinical practices are increasingly focusing on accurate drug usage models provided by laboratory and pharmaceutical professionals to help implement personalized treatment plans. In recent years, the range of SERS applications for monitoring drug metabolism has grown significantly. The first application is the precise quantification of drugs in the body. Benzodiazepines at normal doses have a calming effect, while large doses can lead to acute poisoning, coma, and respiratory arrest, posing a life-threatening risk. Therefore, clinical guidelines set the blood concentration level for these drugs to not exceed 2 μg/ml. Based on this, Zheng et al. developed a SERS monitoring method by first wrapping dopamine on the magnetic Fe_3O_4 surface. The resulting polydopamine stabilized the SERS signal and prevented oxidation of the metal nanoparticles, while maintaining their reduction capacity, allowing the nanoparticles to attach in situ to the surface. They prepared a SERS substrate with multiple "hotspot" structures, as shown in Figure 4a. They also used three-dimensional finite-difference time-domain (FDTD) simulations to model the electric field distribution of different gold nanoparticle sizes, fixing the Fe_3O_4 size at 500 nm and setting gold nanoparticle sizes to 18 nm, 20 nm, 30 nm, and 35 nm. The gaps between these four FPA surfaces were 17, 14, 10, and 0 nm, respectively. The electric field distribution in Figure 4b shows that the FPA-150 with the smallest gap exhibited the best local field enhancement. This was chosen as the substrate for trace detection of benzodiazepines, Estazolam, and diazepam in human serum samples. The results showed that the intensity of the characteristic Raman bands at 1000 cm^{-1} increased with concentration (Figure 4c). The detection limit for single drugs was as low as 50 ng/ml, and for mixed drugs, it was as low as 1 μg/ml, achieving precise quantification [38].

In addition to quantifying drugs in body fluids, intracellular drug metabolism monitoring is an intuitive method for understanding the drug action process. SERS has been developed for this application, but it was found that regular nanoparticle colloids can be captured by cells into vesicles, limiting the detection range. Furthermore, the abundant metabolite signals in the internal environment interfere with the collection of specific signals. Zhang et al. avoided using nanoparticle colloids by selecting roughened nanowires created through a galvanic replacement reaction (GRR), which were inserted into live cells for detection. To read specific target molecule signals near the nanowires, ZIF-8 was applied to the nanowires to evaluate their high selectivity. During intracellular detection, endogenous peptide interference was excluded by using the most common GSH as a reference. The results in Figure 4d showed that small hydrophobic molecules such as 4-MBA could pass through the coating, while large molecules like GSH could not. The mixed SERS spectrum suggested that higher hydrophobic ABT could preferentially adsorb onto ZIF-8, which was detected, proving that ZIF-8 indeed functions as a molecular sieve.

Next, to evaluate the practical application of the nanowire endoscope, irinotecan, an anticancer drug, was selected for study. It is metabolized within cells into smaller and more hydrophobic molecules like SN-38. The ZIF-8 molecular sieve could exclude irinotecan while preferentially detecting SN-38, with characteristic peaks appearing at 1190 cm^{-1}, 1390 cm^{-1}, and 1560 cm^{-1}. Based on this, the AuAgNW@ZIF-8 endoscope was inserted into irinotecan-treated HeLa cell cytoplasm and nucleus, with the specific operation process shown in Figure 4e. The entire process took only a few minutes, and the SERS spectra obtained showed that after 3 hours, SN-38 signals in the cytoplasm became stronger, and after 5 hours, signals were observed in the nucleus. After 24 hours, the nuclear signal disappeared. This process indicates that SN-38 was hydrolyzed in the cytoplasm, and after 5 hours, it diffused into the nucleus to interact with enzymes, losing the SERS signal. This study successfully elucidated the action site and metabolism dynamics of irinotecan in the cell [39].

Exosomes, due to their biocompatibility, can cross cell membranes and have been developed for targeted drug delivery to cancer cells.

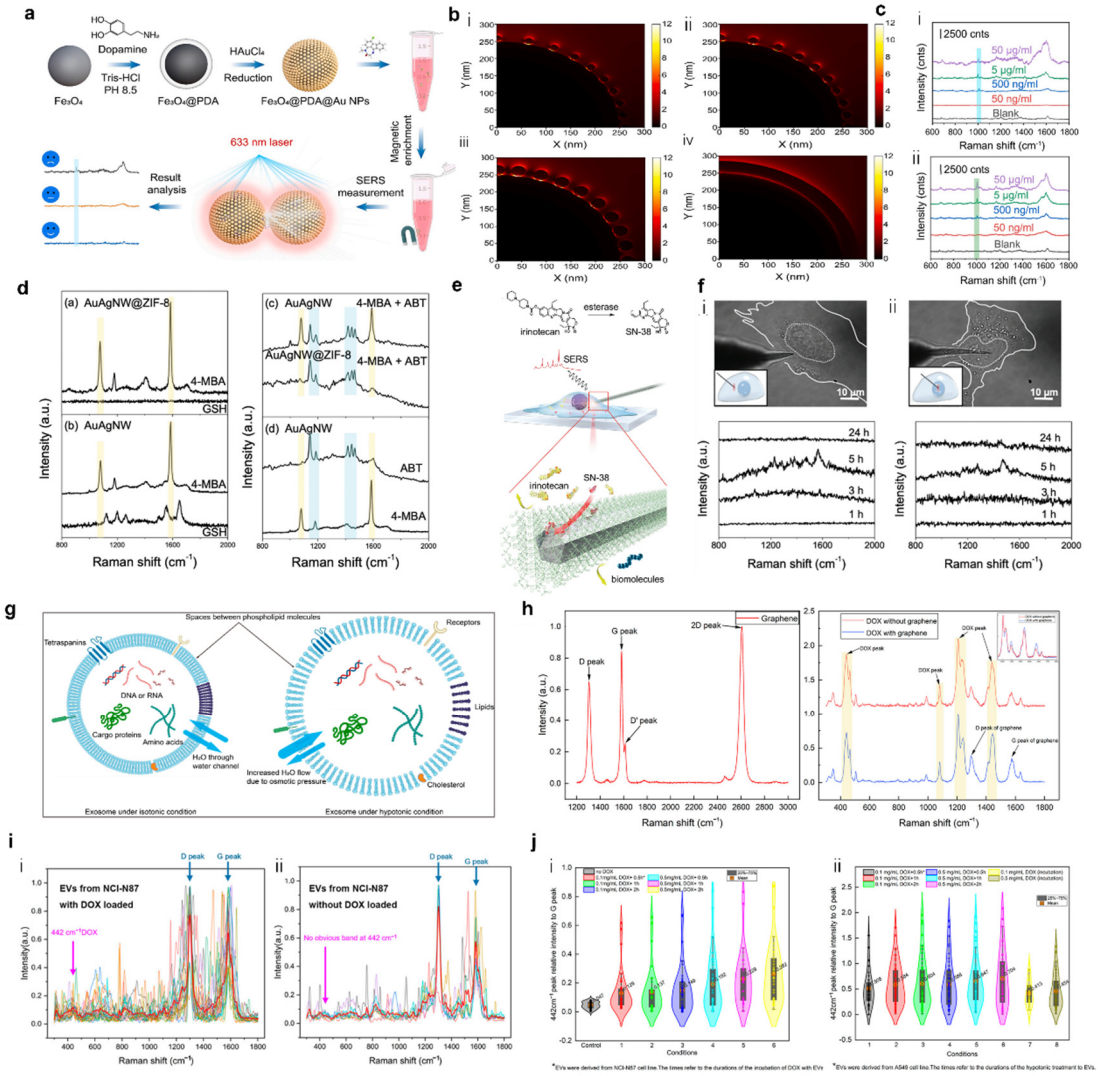


Figure 4. (a) Schematic diagram of Fe_3O_4-polydopamine gold nanoparticle detection for benzodiazepines in serum (b) Electric field distribution maps for FPA-50, FPA-100, FPA-150, and FPA-200 (i-iv) (c) SERS spectra of different concentrations of Estazolam (i) and diazepam (ii) [38] (d) SERS spectra of 4-MBA, GSH, and 4-MBA+ABT mixture detected by AuAgNW@ZIF-8 and AuAgNW (e) Schematic diagram of MOF-coated nanowire endoscope detecting SN-38 (f) Optical microscope images of nanowire endoscope inserted into cytoplasm (i) and nucleus (ii) and their corresponding SERS spectra [39] (g) Hypotonic vs. isotonic exosome membrane states (h) SERS spectra of gold nanoparticle substrate coated with graphene and doxorubicin detection with or without graphene (i) SERS spectra of doxorubicin-loaded (i) and non-loaded exosomes from NCI-N87 cell line (ii) (j) (i) Violin plot of doxorubicin loading in exosomes from NCI-N87 cells at different incubation times and drug concentrations, (ii) Exosomes from A549 cell line under different hypotonic conditions and drug concentrations [40]

When loading drugs into exosomes, there are two strategies: active and passive diffusion loading. The effectiveness of these strategies is verified by evaluating drug-loading efficiency and the impact on exosome characteristics. Liu et al. developed a SERS platform to detect the ability of single exosomes to carry doxorubicin under hypotonic conditions. The feasibility of

this platform arises from the fact that the gap size between the gold nanoparticle hotspots is compatible with the size of a single exosome, suggesting that it may have the ability to detect individual exosomes. As shown in Figure 4g, before the exosome expands and ruptures in the hypotonic solution, the space between phospholipids increases with increasing osmotic pressure. This phenomenon can be used as a time window for drug loading. Unlike other studies, this paper covered the gold nanoparticle substrate with graphene, which served as an internal reference standard to eliminate signal intensity fluctuations caused by uneven hotspot distribution. Figure 4h shows the SERS spectrum of the graphene-coated substrate. The characteristic Raman peaks of D (1304 cm^{-1}), G (1582 cm^{-1}), D' (1613 cm^{-1}), and 2D (2606 cm^{-1}) confirm the presence of monolayer graphene, and both graphene and doxorubicin peaks can be simultaneously excited without interference. After confirming the successful fabrication of the substrate, exosomes were induced to dry onto the SERS substrate and the G peak of graphene was used for calibration, with the I_{DOX}/I_G ratio used to quantify doxorubicin concentration, enabling drug loading quantification at the single exosome level. The exosome detection from the NCI-N87 cell line in Figure 4i showed that SERS spectra from the drug-loaded group clearly observed characteristic Raman shifts of doxorubicin at 442 cm^{-1}. Furthermore, Figure 4j suggests that compared to conventional incubation, exosomes treated with hypotonic solutions showed higher doxorubicin loading efficiency (higher average relative intensity), but the effect was limited. Further analysis showed that even under the same conditions, there was heterogeneity in drug loading among exosomes. The establishment of this platform is expected to facilitate extensive cell culture experiments in future studies. As seen, SERS technology is highly versatile in drug research applications [40].

4. Summary and Outlook

SERS technology has shown unique advantages in the field of drug and metabolite detection, making significant progress in recent years. Through plasmonic resonance phenomena, the Raman signals of target molecules are amplified by more than a million times, enabling high-sensitivity detection of trace small molecules. Compared to traditional detection methods, SERS spectral peaks, which are narrow, can provide molecular-level "fingerprint" structural information, offer high-throughput multiplex detection capabilities, and have strong resistance to photobleaching and water interference, making them especially suitable for the analysis of complex biological samples. However, SERS is not perfect and still faces multiple challenges. For example, molecular detection has inherent limitations, as only specific functional groups can generate strong Raman signals. Substances with similar structures can severely interfere with detection specificity in complex biological samples. Additionally, poor quantitative reproducibility remains a long-term issue. The root cause lies in the difficulty of ensuring substrate uniformity, as etched substrates are expensive and colloidal substrates lack controllability. Furthermore, differences in instrument performance and processing procedures between laboratories make it difficult to replicate research results. Lastly, there is a lack of standardization in sample preprocessing. A universal consensus has not yet been established in the field, and a balance between preprocessing complexity and detection efficiency needs to be achieved.

Looking to the future, the development of SERS in drug and metabolite detection will focus on three major directions. First is the development of high-performance substrate materials, expanding from precious metals to emerging systems like semiconductors and MOF composites. This includes precisely constructing "hotspot" regions, developing self-assembled arrays, and using template methods to create ordered structures, ensuring uniform hotspot distribution. At the same time, efforts will be made to develop low-cost, scalable manufacturing processes to move substrates from laboratory customization to

industrialization. Second is the establishment of standardized technical protocols, which is key for clinical translation. Unified standards need to be formed for sample preprocessing, substrate evaluation, detection procedures, and data processing. Differential guidelines should be created for different sample types, and cross-laboratory multi-center validation should be carried out. Third is the deep integration of AI-assisted spectral analysis. Large language models open new directions for spectral interpretation, and they may help overcome the challenges of quantitative analysis of mixtures. With the miniaturization, cost reduction, and intelligence of portable Raman systems, and the collaborative progress in the three directions mentioned above, SERS will move out of the laboratory and play a significant role in therapeutic drug monitoring, personalized medicine, and at-home immediate testing scenarios, providing strong support for precision medicine from molecular recognition to clinical decision-making.

References

[1] Giera, M., Yanes, O., & Siuzdak, G. (2022). Metabolite discovery: Biochemistry's scientific driver. *Cell Metabolism*, *34*(1), 21–34. https://doi.org/10.1016/j.cmet.2021.12.004.

[2] Rigoulet, M., Bouchez, C. L., Paumard, P., Ransac, S., Cuvellier, S., Duvezin-Caubet, S., Mazat, J. P., & Devin, A. (2020). Cell energy metabolism: An update. *Biochimica et Biophysica Acta (BBA)-Bioenergetics*, *1861*(11), 148276. https://doi.org/10.1016/j.bbabio.2020.148276.

[3] Tonack, S., Tang, C., & Offermanns, S. (2013). Endogenous metabolites as ligands for G protein-coupled receptors modulating risk factors for metabolic and cardiovascular disease. *American Journal of Physiology-Heart and Circulatory Physiology*, *304*(4), H501–H513. https://doi. org/10. 1152/ ajpheart. 00642. 2012.

[4] Hornisch, M., & Piazza, I. (2025). Regulation of gene expression through protein-metabolite interactions. *NPJ Metabolic Health and Disease*, *3*(1), 7. https://doi.org/10.1038/s44187-025-00007-2.

[5] Schvartzman, J. M., Thompson, C. B., & Finley, L. W. S. (2018). Metabolic regulation of chromatin modifications and gene expression. *Journal of Cell Biology*, *217*(7), 2247–2259. https://doi.org/10. 1083/ jcb.201803061.

[6] Newgard, C. B. (2017). Metabolomics and metabolic diseases: Where do we stand? *Cell Metabolism*, *25*(1), 43–56. https://doi.org/10.1016/j.cmet.2016.12.006.

[7] Sieckmann, T., & Kirschner, K. M. (2020). Polyamines, metabolites and metabolomics. *Acta Physiologica*, *229*(3), e13480. https://doi.org/10.1111/apha.13480.

[8] Tang, Y., Li, Z., Lazar, L., Fang, Z., Tang, C., & Zhao, J. (2019). Metabolomics workflow for lung cancer: Discovery of biomarkers. *Clinica Chimica Acta*, *495*, 436–445. https://doi.org/10. 1016/j. cca. 2019. 05. 041.

[9] Ketavarapu, V., Addipilli, R., Ragi, N., Pallerla, P., Simhadri, V., Manne, S., Sannapaneni, K., Aslam, M., Talukadar, R., Ch, V. D., Gv, R., Amanchy, R., Reddy, D. N., Sripadi, P., & Sasikala, M. (2024). Plasma metabolite profiling identifies nondiabetic chronic pancreatitis patients with metabolic alterations progressing to prediabetes before HbA1c. *Clinical and Translational Gastroenterology*, *15*(6), e1. https://doi.org/10.14309/ctg.0000000000000741.

[10] Schmidt, D. R., Patel, R., Kirsch, D. G., Lewis, C. A., Vander Heiden, M. G., & Locasale, J. W. (2021). Metabolomics in cancer research and emerging applications in clinical oncology. *CA: A Cancer Journal for Clinicians*, *71*(4), 333–358. https://doi.org/10.1002/caac.21689.

[11] Kumar, R., Mishra, A., Gautam, P., Feroz, Z., Vijayaraghavalu, S., Likos, E., Shukla, G., & Kumar, M. (2022). Metabolic pathways, enzymes, and metabolites: Opportunities in cancer therapy. *Cancers*, *14*(21), 5268. https://doi.org/10.3390/cancers14215268.

[12] Sagini, K., Urbanelli, L., Buratta, S., Emiliani, C., & Llorente, A. (2023). Lipid biomarkers in liquid biopsies: Novel opportunities for cancer diagnosis. *Pharmaceutics*, *15*(2), 437. https://doi.org/ 10. 3390/ pharmaceutics15020437.

[13] Broadfield, L. A., Pane, A. A., Talebi, A., Swinnen, J. V., & Fendt, S.-M. (2021). Lipid metabolism in cancer: New perspectives and emerging mechanisms. *Developmental Cell*, *56*(10), 1363–1393. https://doi.org/ 10.1016/ j. devcel.2021.04.025.

[14] Solon-Biet, S. M., Cogger, V. C., Pulpitel, T., Wahl, D., Clark, X., Bagley, E. E., Gregoriou, G. C., Senior, A. M., Wang, Q.-P., Brandon, A. E., Perks, R., O'Sullivan, J., Koay, Y. C., Bell-Anderson, K., Kebede, M., Yau, B., Atkinson, C., Svineng, G., Dodgson, T., Wali, J. A., Piper, M. D. W., Juricic, P., Partridge, L., Rose, A. J., Raubenheimer, D., Cooney, G. J., Le Couteur, D. G., & Simpson, S. J. (2019). Branched-chain amino acids impact health and lifespan indirectly via amino acid balance and appetite control. *Nature Metabolism*, *1*(5), 532–545. https://doi.org/10.1038/s42255-019-0067-8.

[15] Kelly, B., & Pearce, E. L. (2020). Amino assets: How amino acids support immunity. *Cell Metabolism*, *32*(2), 154–175. https://doi.org/10.1016/j.cmet.2020.06.010.

[16] Jager, N. G. L., van Hest, R. M., Lipman, J., Taccone, F. S., & Roberts, J. A. (2016). Therapeutic drug monitoring of anti-infective agents in critically ill patients. *Expert Review of Clinical Pharmacology*, *9*(7), 961–979. https://doi.org/10.1080/17512433.2016.1179585.

[17] Zhang, Z., & Tang, W. (2018). Drug metabolism in drug discovery and development. *Acta Pharmaceutica Sinica B*, *8*(5), 721–732. https://doi.org/10.1016/j.apsb.2018.04.002.

[18] Fleischmann, M., Hendra, P. J., & McQuillan, A. J. (1974). Raman spectra of pyridine adsorbed at a silver electrode. *Chemical Physics Letters*, *26*(2), 163–166. https://doi.org/10.1016/0009-2614(74)85388-1.

[19] Huang, Z., Peng, J., Xu, L., & Liu, P. (2024). Development and application of surface-enhanced Raman scattering (SERS). *Nanomaterials*, *14*(17), 1417. https://doi.org/10.3390/nano14171417.

[20] Pence, I., & Mahadevan-Jansen, A. (2016). Clinical instrumentation and applications of Raman spectroscopy. *Chemical Society Reviews*, *45*(7), 1958–1979. https://doi.org/10.1039/C5CS00902J.

[21] Wang, W., & Vikesland, P. J. (2023). Metabolite-mediated bacterial antibiotic resistance revealed by surface-enhanced Raman spectroscopy. *Environmental Science & Technology*, *57*(36), 13375–13383. https://doi.org/10.1021/acs.est.3c02394.

[22] Yu, H.-J., Jang, E., Woo, A., Han, I. W., Jeon, H. G., Linh, V. T. N., Park, S.-G., Jung, H. S., & Lee, M.-Y. (2024). Cancer screening through surface-enhanced Raman spectroscopy fingerprinting analysis of urinary metabolites using surface-carbonized silver nanowires on a filter membrane. *Analytica Chimica Acta*, *1292*, 342233. https://doi.org/10.1016/j.aca.2024.342233.

[23] Han, X. X., Rodriguez, R. S., Haynes, C. L., Ozaki, Y., & Zhao, B. (2022). Surface-enhanced Raman spectroscopy. *Nature Reviews Methods Primers*, *1*(1), 87–103. https://doi.org/10.1038/s43586-022-00087-y.

[24] Zong, C., Xu, M., Xu, L.-J., Wei, T., Ma, X., Zheng, X.-S., Hu, R., & Ren, B. (2018). Surface-enhanced Raman spectroscopy for bioanalysis: Reliability and challenges. *Chemical Reviews*, *118*(10), 4946–4980. https://doi.org/10.1021/acs.chemrev.8b00035.

[25] Ding, S.-Y., You, E.-M., Tian, Z.-Q., & Moskovits, M. (2017). Electromagnetic theories of surface-enhanced Raman spectroscopy. *Chemical Society Reviews*, *46*(13), 4042–4076. https://doi.org/ 10.1039/ C7CS00237A.

[26] Wang, X., Huang, S.-C., Hu, S., Yan, S., & Ren, B. (2020). Fundamental understanding and applications of plasmon-enhanced Raman spectroscopy. *Nature Reviews Physics*, *2*(5), 253–271. https://doi.org/ 10. 1038/ s42254-020-0181-9.

[27] Zrimsek, A. B., Chiang, N., Mattei, M., Zaleski, S., McAnally, M. O., Chapman, C. T., Henry, A.-I., Schatz, G. C., & Van Duyne, R. P. (2016). Single-molecule chemistry with surface- and tip-enhanced Raman spectroscopy. *Chemical Reviews*, *117*(11), 7583–7613. https://doi.org/ 10.1021/ acs. chemrev. 6b00552.

[28] Chang, H., Hur, W., Kang, H., & Jun, B.-H. (2025). In vivo surface-enhanced Raman scattering techniques: nanoprobes, instrumentation, and applications. *Light: Science & Applications*, *14*(1), 79. https:// doi. org/ 10.1038/s41377-025-00915-6.

[29] Bock, S., Choi, Y.-S., Kim, M., Yun, Y., Pham, X.-H., Kim, J., Seong, B., Kim, W., Jo, A., Ham, K.-M., Lee, S. G., Lee, S. H., Kang, H., Choi, H. S., Jeong, D. H., Chang, H., Kim, D.-E., & Jun, B.-H. (2022). Highly

sensitive near-infrared SERS nanoprobes for in vivo imaging using gold-assembled silica nanoparticles with controllable nanogaps. *Journal of Nanobiotechnology*, *20*(1), 130. https:// doi. org/ 10.1186/s12951-022-01328-9.

[30] Wang, C., Xu, J., Weng, G., Li, J., Zhu, J., & Zhao, J. (2025). Gold nanorod in silver tetrahedron: Cysteamine mediated synthesis of SERS probes with embedded internal markers for AFP detection. *Analytica Chimica Acta*, *1340*, 343667. https://doi.org/10.1016/j.aca.2025.343667.

[31] Zhao, Y., Zou, Y., Zhao, W., Huang, C., Zhou, Y., Li, G., Li, M., Jin, S., & Jiang, L. (2026). MXene-Au@Ag hydrogel patch as a wearable SERS sensor for multiplexed sweat analysis of uric acid, creatinine, and pH. *ACS Sensors*, *11*(2), 1592–1602. https://doi.org/10.1021/acssensors.5c02116.

[32] Cai, C., Liu, Y., Zhang, Z., Tian, T., Wang, Y., Wang, L., Zhang, K., & Liu, B. (2023). Activity-based self-enriched SERS sensor for blood metabolite monitoring. *ACS Applied Materials & Interfaces*, *15*(4), 4895–4902. https://doi.org/10.1021/acsami.2c20231.

[33] Dong, P., Xiong, S., Gong, Y., Wang, C., Li, X., & Wu, X. (2026). SERS-based pump-free microfluidic chip sensor for immunoassays of the myocardial injury marker CK-MB. *Sensors and Actuators B: Chemical*, *451*, 139397. https://doi.org/10.1016/j.snb.2026.139397.

[34] Hu, W., Ye, S., Zhang, Y., Li, T., Zhang, G., Luo, Y., Mukamel, S., & Jiang, J. (2019). Machine learning protocol for surface-enhanced Raman spectroscopy. *The Journal of Physical Chemistry Letters*, *10*(20), 6026–6031. https://doi.org/10.1021/acs.jpclett.9b02255.

[35] Khondakar, K. R., Mazumdar, H., Das, S., & Kaushik, A. (2025). Machine learning (ML)-assisted surface-enhanced raman spectroscopy (SERS) technologies for sustainable health. *Advances in Colloid and Interface Science*, *344*, 103594. https://doi.org/10.1016/j.cis.2025.103594.

[36] Zhu, B., Chen, J., Wang, B., Zhou, H., Xiao, R., Gao, Z., & Wang, Y. (2025). Label-free SERS platform assisted by machine learning for multi-target detection and physiological state classification in sweat. *Analytical Chemistry*, *97*(38), 20834–20842. https://doi.org/10. 1021/acs. analchem. 5c02413.

[37] Shafique, H., Rehman, A., Nawaz, H., Majeed, M. I., Alshammari, A., Albekairi, N. A., Ali, A., Shahzadi, A., Yaseen, S., Noor Ul, S., Khalil, M. Z., Yousaf, A., Ali, M., Hussain, M., & Wasim, M. (2025). SERS-based profiling of cholesterol and triglycerides in blood serum samples of lipid metabolic disorders using PCA and PLSR. *Plasmonics*, *20*(10), 9145–9162. https://doi.org/10.1007/s11468-025-01893-1.

[38] Zheng, D., Zhang, X., Zhang, Y., Fan, W., Zhao, X., Gan, T., Lu, Y., Li, P., & Xu, W. (2023). In situ construction of Fe_3O_4@PDA@Au multi hotspot SERS probe for trace detection of benzodiazepines in serum. *Spectrochimica Acta Part A: Molecular and Biomolecular Spectroscopy*, *300*, 122897. https:// doi. org/ 10.1016/j.saa.2023.122897.

[39] Zhang, Q., Murasugi, T., Watanabe, K., Wen, H., Tian, Y., Ricci, M., Rocha, S., Inose, T., Kasai, H., Taemaitree, F., Uji-i, H., Hirai, K., & Fortuni, B. (2023). Selective detection of intracellular drug metabolism by metal-organic framework-coated plasmonic nanowire. *Advanced Optical Materials*, *11*(22), 2300856. https://doi.org/10.1002/adom.202300856.

[40] Liu, J., Srivastava, S., Li, T., Moujane, F., Lee, J. Y., Chen, Y., Liu, H., Deng, S. X., & Xie, Y.-H. (2025). On the feasibility of SERS-based monitoring of drug loading efficiency in exosomes for targeted delivery. *Biosensors*, *15*(3), 141. https://doi.org/10.3390/bios15030141.